THE LITHIUM–SODIUM THIOCHROMITE ALL-SOLID-STATE HIGH TEMPERATURE SECONDARY CELL

PETR NOVÁK*
J. Heyrovský Institute of Physical Chemistry and Electrochemistry, Czechoslovak Academy of Sciences, 182 23 Prague 8 (Czechoslovakia)

YORDAN GERONOV and BOGDANA PURESHEVA
Central Laboratory of Electrochemical Power Sources, Bulgarian Academy of Sciences, Sofia 1040 (Bulgaria)

PETR PODHÁJECKÝ and BŘETISLAV KLÁPŠTĚ
J. Heyrovský Institute of Physical Chemistry and Electrochemistry, Czechoslovak Academy of Sciences, 182 23 Prague 8 (Czechoslovakia)

PETIA ZLATILOVA
Central Laboratory of Electrochemical Power Sources, Bulgarian Academy of Sciences, Sofia 1040 (Bulgaria)

(Received December 20, 1988; in revised form July 13, 1989)

Summary

The electrochemical performance of the lithium–sodium thiochromite solid polymer electrolyte cell was characterized in the 120 °C - 140 °C temperature range by using galvanostatic cycling and electrochemical impedance measurements. A similar cell with an Li(Al) negative electrode was also studied but no substantial differences between the systems were found.

Cells utilizing pressed composite electrodes performed better than those with foil composite electrodes. More than 100 cycles were reached with $Li/P(EO)_8 \cdot LiClO_4/Na_xV_yCrS_2$ cells. At 140 °C, a coulombic capacity of 80 - 120 mA h g^{-1} $Na_xV_yCrS_2$ was achieved during cycling.

The electrode kinetics were studied by potential step and a.c. impedance measurements. It is shown that the cell performance is limited by slow lithium diffusion in the grains of $Na_xV_yCrS_2$.

During cycling, the active material utilization decreases and the internal resistance of the cell is increased by a factor of five.

The self-discharge losses were found to be about 2 - 3% per day.

Introduction

Some types of all-solid-state rechargeable electrochemical cells with solid polymer electrolytes are probably not far from being produced commercially [1 - 3]. Such cells incorporate a lithium or lithium-based negative electrode and a composite positive electrode containing vanadium oxides V_2O_5, V_6O_{13}, V_2O_4, titanium disulfide, TiS_2, or other inorganic insertion compounds, as the electroactive material. Although some room temperature solid polymer electrolytes are under development [1, 4 - 12], current elec-

*Author to whom correspondence should be addressed.

0378-7753/89/$3.50

trolytes formed by a mixture of commercially available poly(ethylene oxide) (PEO) and a lithium salt (for example, $LiClO_4$ or $LiCF_3SO_3$) need temperatures of 70 °C - 150 °C [1 - 3].

The properties of the lithium–polymer electrolyte interface were studied recently [13 - 20]. Generally, the cycling of lithium on Li or Al substrates is not a serious problem because a polarization of less than 100 mV is typical for this type of interface [1, 18]. At 110 °C, the interfacial resistance between the lithium or Li(Al) electrode and PEO/$LiClO_4$ electrolyte was found to be about 7 Ω [19].

The highest ionic conductivity in the 70 °C - 150 °C temperature region was found for a PEO/$LiClO_4$ eutectic (8:1) mixture [21]. Above 100 °C, high conductivity values (10^{-4} - 10^{-3} S cm^{-1}) are reached over the composition range 8:1 - 48:1, where the elastomeric phase alone exists.

The redox stability domain of PEO-based solid electrolytes is believed to be suitable for practical electrochemical couples [22]. The polymer is stable against lithium metal but this is kinetic rather than thermodynamic, being associated with the formation of a passivating film [13, 22]. Below 140 °C, the voltage stability window is believed to be in excess of 3.3 V for PEO/$LiCF_3SO_3$ electrolytes [22].

The most complicated constituent of the all-solid-state cell is the positive composite electrode [23]. This is an agglomeration of small particles of an electrode-active material bound together with a soft, solid electrolyte. Electronic conduction is ensured by the addition of graphite or acetylene black to the composite electrode [1 - 3] or by the use of an electronically conductive, organic, electrode-active material [24].

Both the insertion electrode-active material and the solid polymer electrolyte exist in many phases depending on their composition. Further, both the grain size and the method of manufacture influence electrode performance. Thus, the reproducibility of the electrochemical parameters of the composite electrodes is rather poor [3].

Although the number of papers dealing with the polymer-electrolyte-based all-solid-state batteries is increasing, there is still a lack of fundamental information. The characterization of thick, composite electrodes is important for their practical use. Furthermore, data on composite electrodes based on compounds other than vanadium oxides or titanium disulfide are unknown. There is a group of insertion materials, sodium thiochromites, with excellent electrochemical properties, giving a coulombic capacity of about 200 mA h g^{-1} when used in lithium cells with liquid electrolytes [25]. We selected the best material of this group, $Na_{0.1}Cr_{0.85}V_{0.15}S_2$, and constructed a Li/solid polymer electrolyte/$Na_xV_yCrS_2$ cell. The characteristics of this cell are presented here.

Experimental

All electrochemical measurements were performed using a two-electrode system with a lithium or Li(Al) negative counter-electrode. The

potentials of these have been shown to be nearly constant during measurements of composite electrodes with solid polymer electrolytes [1, 18]. The two-electrode system was therefore considered to be sufficient in our work. The electrolyte consisted of a 100 μm-thick layer of poly(ethylene oxide) (PEO, Aldrich, mol. wt. 5 000 000, used as-received) containing $LiClO_4$ in a ratio of 1 molecule of the salt to 8 monomeric units, *i.e.*, $P(EO)_8 \cdot LiClO_4$. Bubble- and hole-free solid electrolyte foils were prepared by casting a 1 vol.% solution of the PEO containing the proper amount of the salt, in acetonitrile onto a PTFE foil. The solvent was allowed to evaporate slowly at 25 °C. The resulting films were vacuum dried for one day at 120 °C and then left at least one month in a dry (to less-than 20 ppm H_2O) argon atmosphere at room temperature. The composition $P(EO)_8 \cdot LiClO_4$ was chosen because it gave the highest ionic conductivity over the working temperature (120 °C - 140 °C) [21].

The positive electrode active material, $Na_{0.1}Cr_{0.85}V_{0.15}S_2$ (denoted in the text as $Na_xV_yCrS_2$), was synthesized as described in ref. 25. To prepare the composite electrodes the electrode active material, $Na_xV_yCrS_2$, was first mixed in the dry state with the desired amount of acetylene black (P1042, Stickstoffwerke Piesteritz, GDR). The mixture was then wetted with acetonitrile using ultrasonic treatment (5 min), and the desired amount of a solution of 1 vol.% $P(EO)_8 \cdot LiClO_4$ in acetonitrile was added. The resulting slurry was mixed with a magnetic stirrer for 8 h during which time it received several, 5 min, ultrasonic treatments.

After casting the slurry onto a PTFE foil the acetonitrile was allowed to slowly evaporate at 25 °C. The resulting foils of electrode composite were vacuum dried for 3 h at 60 °C and then 8 h at 120 °C and stored under an argon atmosphere in the dry box. Just before use, the foils were pressed in the box at about 10 MPa between stainless steel pistons, and circular electrodes (geometric area 1.77 cm^2, about 100 μm thick) were cut from the foil. These electrodes, denoted in this paper as "foil electrodes", contained 45 wt.% (about 7 mg) active electrode material, 5 wt.% acetylene black, and 50 wt.% $P(EO)_8 \cdot LiClO_4$. The described method of foil electrode preparation is similar to those commonly used in other laboratories [1 - 3] although the proportions differ.

For thicker electrodes the acetonitrile was evaporated from the slurry of $Na_xV_yCrS_2$, C, and $P(EO)_8 \cdot LiClO_4$ at 25 °C. The resulting material was heated at 120 °C under vacuum for 3 h and homogenized. The dry mix was pressed at 600 MPa to form approximately 0.24 mm-thick discs of 1.77 cm^2 area, containing 40 wt.% $Na_xV_yCrS_2$ (about 18 mg), 40 wt.% acetylene black, and 20 wt.% $P(EO)_8 \cdot LiClO_4$. The electrodes were vacuum dried at 120 °C for 4 h and stored in an argon-filled dry box prior to use. They are referred to below as "pressed electrodes". The theoretical coulombic capacity, C_t, was calculated from the $Na_xV_yCrS_2$ content, assuming that at 100%, $C_t = 196$ mA h g^{-1}.

The electrochemical cells were assembled in a glove box according to the button cell structure [26]. Lithium metal, freshly scraped with a scalpel,

was pressed into a stainless steel die, the circular lithium surface was covered with one sheet of the solid electrolyte, and the composite positive electrode was placed on the top of the structure. The electrode assembly, spring loaded to about 2 kg cm^{-2} between stainless steel current collectors, was hermetically sealed with a PTFE foil ready for testing. Some experiments were performed with the Li(Al) negative electrode, prepared according to ref. 27, instead of pure Li.

The electrochemical impedances were measured by the standard procedure in the potentiostatic mode using 1 mV a.c. perturbation. The internal resistance, R_i, of the cell was evaluated using currents between 5 μA and 1 mA; the voltage was recorded 10 s after switching on the current.

Comments on the preparation of solid electrolyte foils

To prepare the solid polymer electrolyte we selected a 1 vol.% solution of $P(EO)_8 \cdot LiClO_4$ in acetonitrile. This has a relatively high viscosity, but still allows the gas bubbles to escape to the surface after the solution is cast. The acetonitrile was evaporated at 25 °C because, at higher temperatures, bubble formation in the bulk of the solution was observed. The evaporation must proceed very slowly (1 - 2 days for 1 cm of solution) in order to obtain good quality homogeneous films. Good results were also obtained when lower molecular weight PEO (600 000) was used instead of 5 000 000.

Drying the film must be started within a few days of evaporation of the solvent because films stored in air slowly deteriorate — the viscosity of the films decreased with time and they changed gradually to a brownish colour.

Long-term cycling was found to be impossible with films dried at 25 °C in the dry argon glove box for up to three months, due to internal shorts, probably caused by lithium dendrites formed during charging. It has been reported [28] that at 25 °C residual water forms a complex with $LiClO_4$ through hydrogen bonding. Furthermore, water may also form hydrogen bonds to oxygen atoms on the polymer backbone [28]. We believe, therefore, that this water and/or the rest of the acetonitrile were responsible for the assumed dendrite formation. As the temperature is raised above 100 °C the hydrogen bonds are broken [28] and no water remains in the solid electrolyte under vacuum [29]. We therefore heated the foils (3 h at 60 °C followed by 8 h at 120 °C) under vacuum and dendrite shorts were very seldom observed.

Foils dried at elevated temperature are soft and sticky. After some weeks of storage at 25 °C under an argon atmosphere the films no longer stick and their mechanical properties are excellent for subsequent cell construction; we observed no difference between the electrochemical properties of the cells prepared with the fresh films and those using aged, solid electrolyte films.

Results and discussion

Cells with the Li(Al) electrode

Secondary electrochemical cells with solid polymer electrolytes usually utilize pure Li or Na metal or Li(Al) alloy as the negative electrode [1, 2, 30]. We performed some comparative studies on our positive electrode material using both lithium-based negative electrodes. From the results we concluded that there is no substantial difference in the electrochemical behaviour of either cell type (other than that due to the potential of the Li(Al) electrode being about 300 mV more positive than that of pure lithium, resulting in a lower cell voltage). Typical results, valid for systems with either negative electrode, are presented here for the case of the Li(Al)/$P(EO)_8 \cdot LiClO_4/Na_xV_yCrS_2$ (pressed composite electrode) cell.

Charge and discharge curves for cells cycled galvanostatically are shown in Fig. 1. The cycling profile of the solid polymer electrolyte cell is similar to that described for the corresponding liquid electrolyte cell [25]. The curves are smooth, without steps and plateau — an indication that there is probably only one electrochemical reaction. The cell is capable of relatively high current densities, up to 1.5 mA cm^{-2}, with linear current–load characteristics (Fig. 2). The typical internal resistance of cells after a few cycles is about 120 Ω at 130 °C. The Li(Al) cell can be cycled many times; its cycle performance is similar to that of cells with pure lithium, described below.

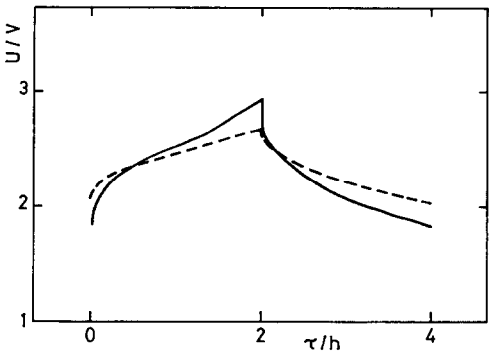

Fig. 1. Typical cycling profiles of the pressed composite electrode in the Li(Al)/$P(EO)_8 \cdot LiClO_4/Na_xV_yCrS_2$ cell. Temperature 130 °C. —— 2 h charge 0.8 mA (50% C_t), 2 h discharge 0.8 mA, cycle number 24, — — — 2 h charge 0.4 mA (25% C_t), 2 h discharge 0.4 mA, cycle number 20.

Comparison of foil and pressed electrodes

For the majority of cycling tests we selected galvanostatic cycling between potential limits. Our preliminary experiments showed that the charging current density should be two to four times lower than the discharging current density and in order to achieve a long cycle life the higher potential limit should not exceed approximately 2.70 V (*versus* Li/Li^+). The reason for this is unclear to us because we successfully cycled some

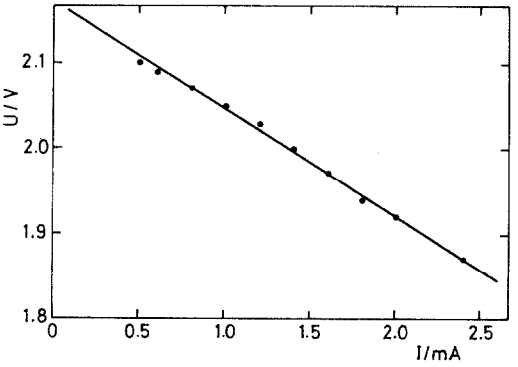

Fig. 2. Current–load characteristics of the pressed composite electrode in the Li(Al)/$P(EO)_8 \cdot LiClO_4/Na_xV_yCrS_2$ cell. Temperature 130 °C, electrode area 1.77 cm^2.

cells to a higher potential limit of up to 3.0 V but the majority failed at potentials above 2.75 V. "Failed cells", if charged galvanostatically further, exhibited an almost constant, noisy voltage of about 2.8 V. Manual current reversal sometimes helped to restore the cell cycling properties but usually the next charging was again unsuccessful.

A possible reason could be partial cell shorting due to dendrite formation caused, for example, by the presence of residual water and/or acetonitrile in the solid electrolyte and/or the positive electrode. Residual solvents could fill some micropores in the PEO (if they exist) thus making liquid electrolyte connections between the electrodes. The ionic conductivity of the liquid phase is higher than that of the solid electrolyte and, during charging, lithium dendrites could grow through such micropores. The cathode active material could also be a source of the problem since oxidation of the solid polymer electrolyte at the limiting potential is possible, perhaps with the catalytic contribution of the $Na_xV_yCrS_2$ discharge products. Similar charging problems were observed with the $Li/P(EO)_8 \cdot LiClO_4/CuO$ [31] and $Li/P(EO)_8 \cdot LiClO_4/(CS_x)_n$ cells [32] but never with the $Li/P(EO)_8 \cdot LiClO_4$/polypyrrole [24, 26, 33] system.

Figure 3 shows how the discharge capacity of the $Na_xV_yCrS_2$ pressed positive electrode varies with the cycle number. During the first discharge, 80% - 90% of the theoretical capacity, C_t, is usually delivered by the cell at 120 (±3) °C. Hence, almost one mole of Li^+ ions is inserted into one mole of the $Na_xV_yCrS_2$ crystal lattice. The subsequent charge, however, is only about 40% of C_t at the same temperature and never pulls all the Li^+ ions out of the $Na_xV_yCrS_2$ structure, even at very low current densities. This result is surprising because in liquid electrolytes the charge and discharge cycles are usually equal [25]. In our case, with the solid polymer electrolyte, about one half of the inserted lithium is "lost" in the crystal lattice, where it is inaccessible for subsequent cycling. Slight differences between discharge and charge capacities are still observable during the following cycles, but

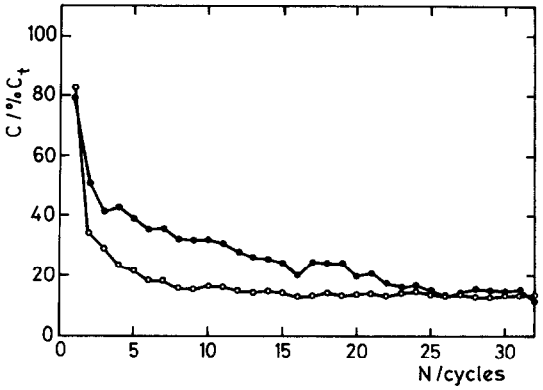

Fig. 3. Typical dependences of the discharge capacities of the $Na_xV_yCrS_2$ pressed and foil positive electrodes on the cycle number. Galvanostatic cycling between 1.20 and 2.70 V (*vs.* Li/Li^+). Temperature 120 °C; Li negative electrode. ●, $-C_t/5$; $+C_t/20$; pressed electrode; ○, $-C_t/10$; $+C_t/40$; foil electrode.

after about five cycles the performance of the cell is stabilized with a significantly lower electrode utilization than in the first cycle.

The active material utilization decreases with cycle number from about 40% C_t (5th cycle) to 20% C_t (at about the 20th cycle) at high discharge rates in the case of the pressed electrode (see Fig. 3). Similar behaviour was also observed with the foil composite electrodes, also shown in Fig. 3, but the cell performance was poorer, even at lower current densities. (The possible reasons for the observed differences are discussed in the next section.) Thus, for practical "coin" cells, thick, pressed composite electrodes are recommended because of both ease of manufacture and better cell performance.

The coulombic efficiency, Q_{disch}/Q_{charge}, during cycling is usually 80 - 100%. It sometimes exceeded 100% — an indication either that some lithium was "lost" in the bulk of the $Na_xV_yCrS_2$ structure or that there were side-reactions, *e.g.*, reduction of H_2O. A coulombic efficiency higher than 100% was also observed with other insertion electrodes having solid polymer electrolytes, *e.g.*, with TiS_2 [1] and V_4O_9 [34] based composites. This problem seems to be, therefore, a rather general one for insertion materials coupled with solid polymer electrolytes.

Characteristics of pressed composite electrodes

The dependence of the discharge capacity of an $Na_xV_yCrS_2$-based, pressed positive electrode on the cycle number for three, nominally identical, cells is shown in Fig. 4. All curves show the same trend with good reproducibility. Comparing our data on pressed electrodes with those of Hooper and North obtained on foil V_6O_{13}-based composite electrodes [3] indicated better reproducibility with the pressed electrodes. We also had problems with the reproducibility of our foil electrodes. We agree with the

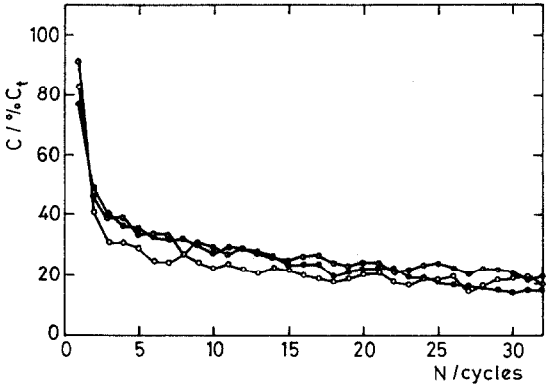

Fig. 4. Dependence of the discharge capacity of the $Na_xV_yCrS_2$ pressed positive electrode on the cycle number. Three nominally identical cells cycled galvanostatically ($-C_t/5$, $+C_t/20$) between 1.40 and 2.70 V (*vs.* Li/Li^+). Temperature 120 °C; Li negative electrode.

conclusions of ref. 3 that the poor reproducibility is caused by non-equilibrium within the cathode during cycling and by changes in the distribution of the components within the composite electrode with time (resulting in the formation of pockets of ionically or electronically insulated material). The intimate mixing, lower soft-solid-electrolyte-content in the composite, and higher pressure used in the electrode preparation, all lead to a lower probability of isolated particle formation. They will also improve the electrochemical performance, and give the pressed composite electrodes a better reproducibility than the foil electrodes.

Another cycling regime is shown in Fig. 5 where the results of galvanostatic cycling (2 h discharge, 2 h charge) are presented. The voltage at the

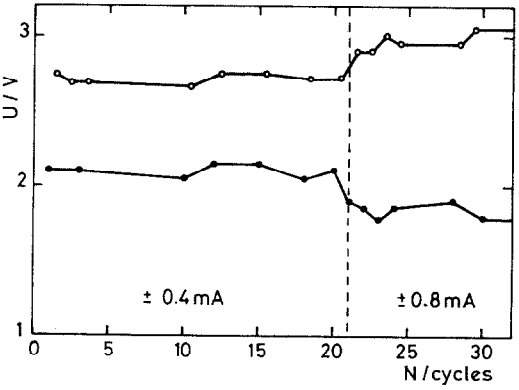

Fig. 5. Dependence of the upper (○) and lower (●) voltage limit (reached at the ends of charging and discharging) on the cycle number, N. $Li(Al)/P(EO)_8 \cdot LiClO_4/Na_xV_yCrS_2$ (pressed electrode) cell. Cycling regime: 2 h discharge, 2 h charge, current ±0.4 mA (corresponding to 18.4% C_t); after cycle number 21 current ±0.8 mA (36.8% C_t). Temperature 120 °C.

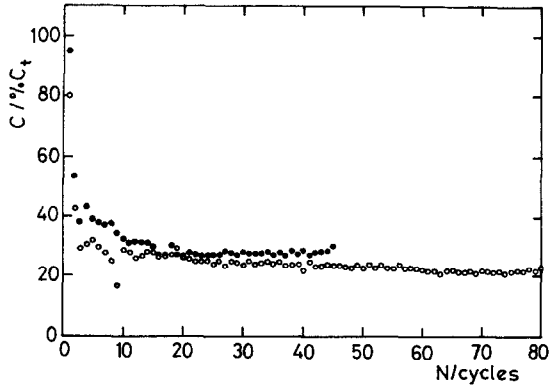

Fig. 6. Dependence of the discharge capacity of the $Na_xV_yCrS_2$ pressed positive electrode on the cycle number. Galvanostatic cycling $-C_t/20$, $+C_t/40$ between: ○, 2.00 V and 2.80 V (*vs.* Li/Li^+); ●, 1.80 and 2.80 V. Temperature 120 °C; Li negative electrode.

end of charge increased by about 12% during cycling while the voltage at the end of discharge fell a similar amount.

The cycle life of sodium thiochromite-based composite electrodes is promising, especially at lower current densities (see, for example, Fig. 6, where the results of 120 °C are presented). After ten cycles, the cell performance is stabilized and the active material utilization reaches about 30% C_t, *i.e.*, about 60 mA h g^{-1} $Na_xV_yCrS_2$. This value slowly decreases during subsequent cycling but more than 100 cycles were reached before the utilization of the active material dropped to 40 mA h g^{-1} (20% C_t). We believe that the cycle life of the $Na_xV_yCrS_2$-based composites can be extended to some hundreds of cycles by improving the sealing of our laboratory cells which usually failed after a few months of heating.

The coulombic capacity of the cell increases significantly with temperature. At 140 °C, 50 - 80% C_t (100 - 160 mA h g^{-1} $Na_xV_yCrS_2$) electrode utilization was reached. At 1 mA cm^{-2} the coulombic capacity at 138 °C was still 100 mA h g^{-1} $Na_xV_yCrS_2$. At 0.25 mA cm^{-2}, the coulombic capacity was close to 160 mA h g^{-1}.

The internal resistance, R_i, of the cell rises significantly with cycle number. At 120 °C it is about 120 Ω during the first ten cycles but rises to 600 Ω during the subsequent 30 cycles. To restore the active material utilization, it is necessary to lower both the charge and discharge current density.

The best electrode utilization was obtained at 140 °C at a current density of 0.28 mA cm^{-2}, namely 40% - 80% C_t for the first 40 cycles. This is very promising for further tests and scaling-up investigations.

Electrode reaction kinetics

The rate-limiting process in insertion-compound-based composite electrodes is the diffusion of lithium within the crystal lattice rather than charge transport in the polymer electrolyte [1]. The rapid capacity decrease

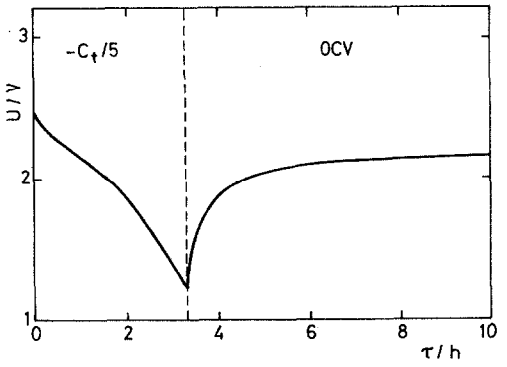

Fig. 7. Galvanostatic ($-C_t/5$) discharge curve for a fresh $Li/P(EO)_8 \cdot LiClO_4/Na_xV_yCrS_2$ cell (pressed electrode) followed by voltage recovery after interruption at 1.2 V. Temperature 120 °C.

during the first few cycles is therefore associated with slow diffusion and/or migration of the inserted Li^+ within the large grains, from where most of it cannot be removed during charging [34]. These conclusions were confirmed during our experiments on sodium thiochromite. Figure 7 shows the voltage recovery after the current interruption at the end of the standard discharge half-cycle, highlighting the slow kinetics of the solid phase processes. The potential equilibration takes many hours — changes below 1 mV h^{-1} are usually reached only after two or three days of heating on open circuit. The diffusion coefficient of the anions in PEO-based solid electrolytes is typically higher than 10^{-8} cm^2 s^{-1} [35]. The observed very slow cell reaction kinetics cannot, therefore, be connected with concentration changes in the solid electrolyte, but rather with changes within the positive electrode. The diffusion coefficient of Li^+ in the $Na_xV_yCrS_2$ crystal lattice is not known, but for the similar compound, $Na_{0.1}CrS_2$, values in the range 10^{-10} - 10^{-11} cm^2 s^{-1} were found [36]. We expect that for the vanadium-doped material $Na_xV_yCrS_2$, this value is of the same order of magnitude. Because of the very slow diffusion of Li^+ in the electrode material only the surface layers of the sodium thiochromite grains are involved in the relatively high-rate cycling used in our experiments.

To quantify the diffusion limitation, we made some potential step experiments. Typical results, in the form of Cottrell plots, are shown in Fig. 8 for both cathodic and anodic 10 mV steps. Theoretically, for a single, semi-infinite diffusion process, only one straight line passing through the origin should be observed. In our case, however, the dependence is more complicated, with two linear portions distinguishable from the curves in Fig. 8.

The current recorded in Fig. 8 does not fall to zero when the duration of the experiment increases; a stable current of about 3 μA flows through the cell under potentiostatic conditions at 120 °C. This can be attributed to compensation of the self-discharge process.

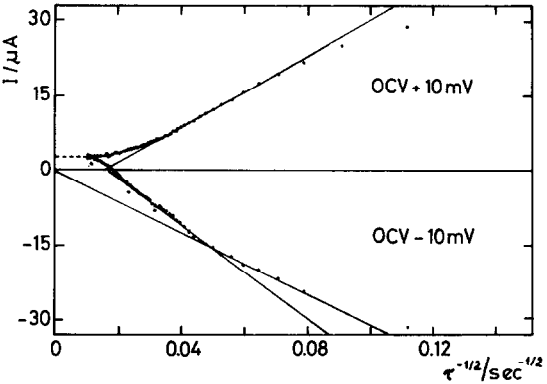

Fig. 8. Typical Cottrell plots for the pressed electrode in the $Li/P(EO)_8 \cdot LiClO_4/Na_xV_yCrS_2$ cell. Temperature 120 °C, cell voltage 2.300 V, potential steps −10 mV and 10 mV from OCV.

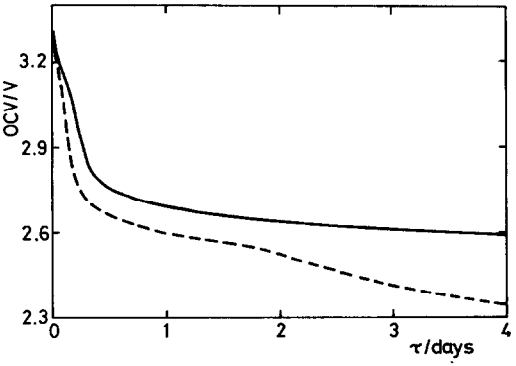

Fig. 9. The OCV–time plot for two $Li/P(EO)_8 \cdot LiClO_4/Na_xV_yCrS_2$ (pressed electrode) fresh cells. Temperature 120 °C.

The fresh cell exhibits a rather high open circuit voltage (OCV) of about 3.4 V at 120 °C (probably due to the presence of impurities or other phases [3]) but it drops rapidly over a few days to 2.6 - 2.7 V (Fig. 9). This is probably the true equilibrium voltage of the undischarged cell. During further heating the OCV drops slowly at a rate of about 1 mV h^{-1} due to self-discharge. The observed current of 3 μA, compensating the self-discharge under potentiostatic conditions, corresponds to about 2 - 3% self-discharge per day, in accordance with the data derived from the OCV curves. This self-discharge rate is comparable with that found for Ni/Cd accumulators [37]. The rate of self-discharge of the $Li/P(EO)_8 \cdot LiClO_4/Na_xV_yCrS_2$ cell is thus acceptable, but much higher than that for ambient-temperature, liquid-electrolyte lithium cells [38].

The reasons for the self-discharge in this and in other all-solid-state polymer-based cells are not fully understood. There is a hypothesis con-

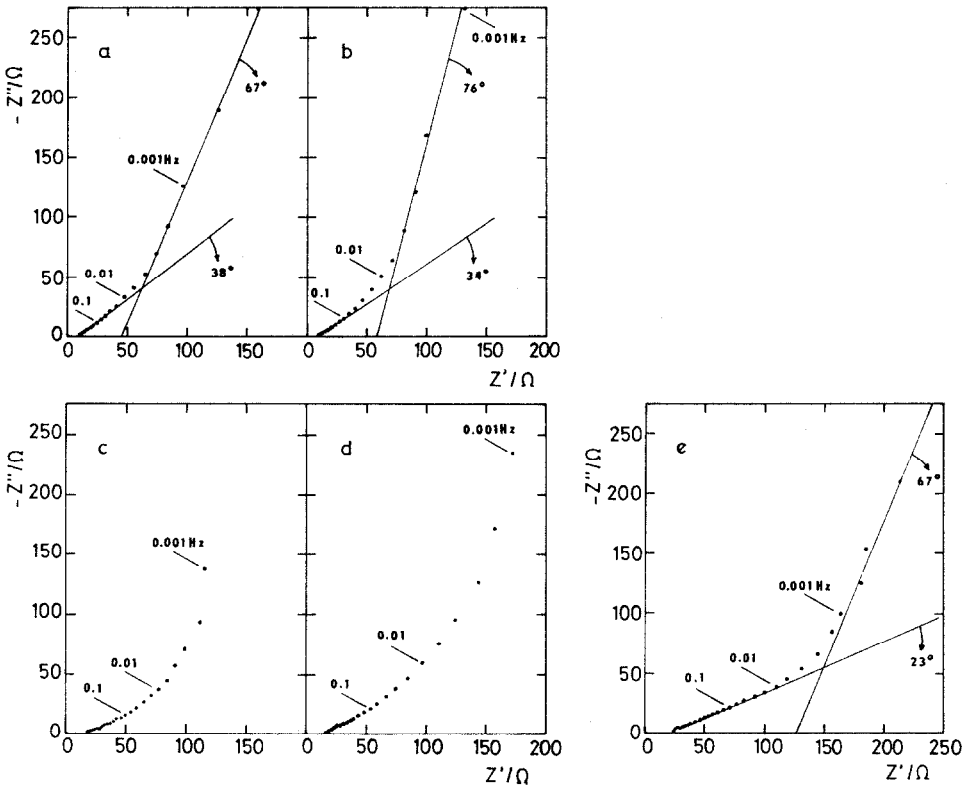

Fig. 10. Typical complex impedance diagrams for: (a) the fresh $Li/P(EO)_8 \cdot LiClO_4/Na_xV_yCrS_2$ cell (pressed electrode) after 4 days on open circuit; (b) the same cell after first galvanostatic discharge ($-C_t/5$) to 1.2 V; (c) the same cell after first galvanostatic charge ($+C_t/20$) to 2.7 V; (d) the same cell after second galvanostatic discharge ($-C_t/5$) to 1.2 V; (e) the same cell after second galvanostatic charge ($+C_t/20$) to 2.7 V. Temperature 120 °C.

cerning a moving redox species transferring the charge between both electrodes [33], but further work on this subject is needed.

Electrochemical impedance studies

In order to understand the cycling behaviour of the cell we performed electrochemical impedance measurements on the $Li/P(EO)_8 \cdot LiClO_4/Na_xV_yCrS_2$ (pressed electrode) cells. The reproducibility of results taken from different cells was excellent. In Figs. 10 and 11 the impedance data for a typical cell are shown.

From the intersection of the impedance curve with the real axis, the sum of ohmic resistances could be estimated. This value, for a fresh cell, is very low — 10 Ω, but rises rapidly during the first few cycles (Fig. 10). There is no significant difference between the values measured at the beginning of cycling in charged and discharged states. After 32 cycles, how-

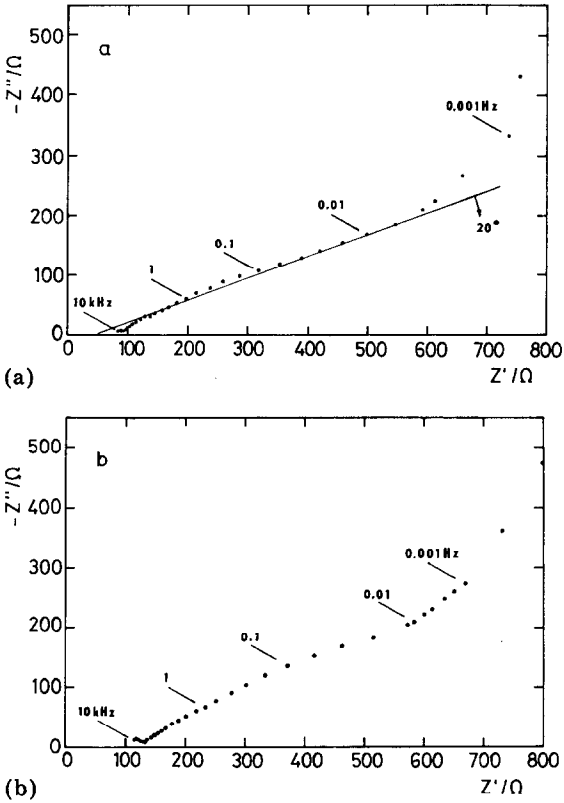

Fig. 11. Typical complex impedance diagrams for the same cell as in Fig. 10 but after 32 galvanostatic cycles ($-C_t/5$; $+C_t/20$), in the charged (a) and discharged (b) state.

ever, the ohmic resistance found for the discharged cell was higher than that of the charged cell (Fig. 11).

The impedance curves in Fig. 10 have a hyperbolic shape, where two Warburg linear portions can be considered as the asymptotes. The impedance curves for the Li/P(EO)$_8$·LiClO$_4$/Li system, Fig. 12, compared with those for an Li/P(EO)$_8$·LiClO$_4$/Na$_x$V$_y$CrS$_2$ cell (Figs. 10 and 11), show a quite different shape and much lower values of the imaginary part of the complex impedance, Z''. The impedance of the Li/P(EO)$_8$·LiClO$_4$/Li cell increases with age when left on open circuit as the passive layer at the lithium/solid electrolyte interface grows [21]. When the Li/P(EO)$_8$·LiClO$_4$/Na$_x$V$_y$CrS$_2$ cell is charged, lithium metal is deposited on the negative side, and thus the interface is renewed. Therefore, for this cell, the main contribution to the overall impedance comes from the positive electrode, which is thus responsible for the observed growth of the overall cell internal resistance, R_i.

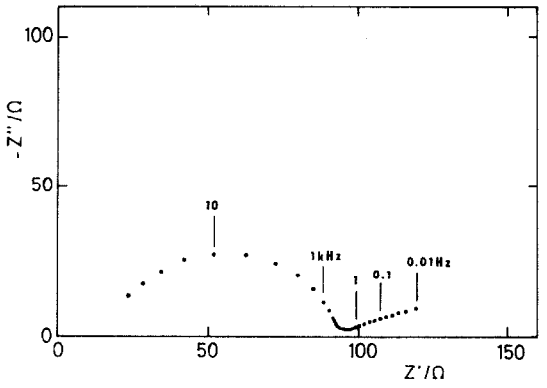

Fig. 12. Typical complex impedance diagram for the system $Li/P(EO)_8 \cdot LiClO_4/Li$. Temperature 120 °C.

Conclusions

(i) There is no substantial difference between either of the possible types of all-solid-state cells utilizing the $Na_xV_yCrS_2$-based composite positive electrode with Li and Li(Al) negative electrodes.

(ii) The performance of the pressed composite electrodes is better than that of the foil composite electrodes.

(iii) The cycle life of sodium thiochromite-based all-solid-state cells is promising — more than 100 cycles were reached.

(iv) At 140 °C, a stable, coulombic capacity of 80 - 120 mA h g^{-1} $Na_xV_yCrS_2$ was reached during cycling. On the basis of the mean discharge potential, 2.5 V *versus* Li/Li^+, and without correction for the Li weight, the specific energy of 250 W h kg^{-1} $Na_xV_yCrS_2$ was calculated, which gives about 100 W h kg^{-1} for a real cell (excluding the case).

(v) The rate-determining step in the cell reaction is probably the slow lithium diffusion within the crystal lattice of $Na_xV_yCrS_2$.

(vi) The active material utilization decreases during cycling. The internal resistance at the end of the cycle life, estimated from the impedance diagrams, rises about five times as compared with the first cycles.

(vii) The self-discharge rate of the sodium thiochromite-based cell is about 2 - 3% per day at 120 °C.

Acknowledgement

The authors are indebted to Dr R. V. Moshtev, CLEHIT, Sofia, for providing samples of vanadium-doped sodium thiochromite.

References

1 M. Gauthier, D. Fauteux, G. Vassort, A. Bélanger, M. Duval, P. Ricoux, J. M. Chabagno, D. Muller, P. Rigaud, M. B. Armand and D. Deroo, *J. Electrochem. Soc., 132* (1985) 1333.
2 M. Gauthier, D. Fauteux, G. Vassort, A. Bélanger, M. Duval, P. Ricoux, J. M. Chabagno, D. Muller, P. Rigaud, M. B. Armand and D. Deroo, *J. Power Sources, 14* (1985) 23.
3 A. Hooper and J. M. North, *Solid State Ionics, 9/10* (1983) 1161.
4 P. M. Blonsky, D. F. Shriver, P. Austin and H. R. Allcock, *J. Am. Chem. Soc., 106* (1984) 6854.
5 M. Hara, K. Shigehara and A. Yamada, *Synth. Met., 18* (1987) 731.
6 P. G. Hall, G. R. Davies, J. E. McIntyre, I. M. Ward, D. J. Bannister and K. M. F. Le Brocq, *Polym. Commun., 27* (1986) 98.
7 A. Bouridah, F. Dalard, D. Deroo, H. Cheradame and J. F. Le Nest, *Solid State Ionics, 15* (1985) 233.
8 J. F. Le Nest, H. Cheradame, F. Dalard and D. Deroo, *J. Appl. Electrochem., 16* (1986) 75.
9 J. F. Le Nest, F. Defendini, A. Gandini, H. Cheradame and J. P. Cohen-Addad, *J. Power Sources, 20* (1987) 339.
10 M. Watanabe, K. Sanui, N. Ogata, T. Kobayashi and Z. Ohtaki, *J. Appl. Phys., 57* (1985) 123.
11 A. Le Méhaute, G. Crepy, G. Marcellin, T. Hamaide and A. Guyot, *Polym. Bull., 14* (1985) 233.
12 N. Kobayashi, M. Uchiyama and E. Tsuchida, *Solid State Ionics, 17* (1985) 307.
13 D. Fauteux, *Solid State Ionics, 17* (1985) 133.
14 F. Bonino, B. Scrosati, A. Selvaggi, J. Evans and C. A. Vincent, *J. Power Sources, 18* (1986) 75.
15 F. Bonino, B. Scrosati and A. Selvaggi, *Solid State Ionics, 18/19* (1986) 1050.
16 F. Bonino, M. Ottaviani, B. Scrosati and G. Pistoia, *J. Power Sources, 20* (1987) 333.
17 S. Morzilli, F. Bonino and B. Scrosati, *Electrochim. Acta, 32* (1987) 961.
18 C. A. C. Sequeira and F. D. S. Marques, *Chemtronics, 1* (1986) 137.
19 M. Armand, *Solid State Ionics, 9/10* (1983) 745.
20 R. Neat, M. Glasse, R. Linford and A. Hooper, *Solid State Ionics, 18/19* (1986) 1088.
21 P. Ferloni, G. Chiodelli, A. Magistris and M. Sanesi, *Solid State Ionics, 18/19* (1986) 256.
22 C. A. C. Sequeira, J. M. North and A. Hooper, *Solid State Ionics, 13* (1984) 175.
23 J. R. Owen, J. Drennan, G. E. Lagos, P. C. Spurdens and B. C. H. Steele, *Solid State Ionics, 5* (1981) 343.
24 P. Novák, O. Inganäs and R. Bjorklund, *J. Electrochem. Soc., 134* (1987) 1341.
25 R. Moshtev, V. Manev, B. Puresheva and G. Pistoia, *Solid State Ionics, 20* (1986) 259.
26 P. Novák, O. Inganäs and R. Bjorklund, *J. Power Sources, 21* (1987) 17.
27 P. Zlatilova, I. Balkanov and Y. Geronov, *J. Power Sources, 24* (1988) 71.
28 E. A. Rietman, M. L. Kaplan and R. J. Cava, *Solid State Ionics, 17* (1985) 67.
29 F. L. Tanzella, W. Bailey, D. Frydrych and H. S. Story, *Solid State Ionics, 5* (1981) 681.
30 K. West, B. Zachau-Christiansen, T. Jacobsen and S. Atlung, *J. Electrochem. Soc., 132* (1985) 3061.
31 P. Novák and P. Podhájecký, *J. Power Sources*, in preparation.
32 L. Kavan, P. Novák and F. P. Dousek, *Electrochim. Acta, 33* (1988) 1605.
33 P. Novák and O. Inganäs, *J. Electrochem. Soc., 135* (1988) 2485.

34 A. Hammouche and A. Hammou, *Electrochim. Acta, 32* (1987) 1451.
35 A. Bouridah, F. Dalard, D. Deroo and M. B. Armand, *J. Appl. Electrochem., 17* (1987) 625.
36 V. Manev, R. V. Moshtev, A. Nassalevska, A. Gushev and G. Pistoia, *Solid State Ionics, 13* (1984) 181.
37 K. Wiesener, J. Garche and W. Schneider, *Elektrochemische Stromquellen,* Akademie-Verlag, Berlin, 1981.
38 J. P. Gabano (ed.), *Lithium Batteries,* Academic Press, London, 1983.